JACS
JOURNAL OF THE AMERICAN CHEMICAL SOCIETY
Article
pubs.acs.org/JACS

Highly Strained Nonclassical Nanotube End-caps. A Single-Step Solution Synthesis from Strain-Free, Non-Macrocyclic Precursors

Damian Myśliwiec, Mateusz Kondratowicz, Tadeusz Lis, Piotr J. Chmielewski, and Marcin Stępień*

Wydział Chemii, Uniwersytet Wrocławski, ul. F. Joliot-Curie 14, 50-383 Wrocław, Poland

Supporting Information

ABSTRACT: Nonclassical nanotube end-caps have been constructed from strain-free heterocyclic precursors using a one-step synthetic procedure, involving multiple nickel-mediated Ullmann couplings. These systems consist of tubular macrocyclic sections that are tightly capped on one side with a bridging benzene ring, forming deep, chemically accessible cavities. The end-caps are characterized by exceptionally high internal strain energies reaching 144 kcal/mol. The optical absorption and emission properties of these molecules show a marked dependence on conjugation length and geometrical factors. The mechanism of end-cap formation, investigated using DFT calculations, relies on precise timing of transmetalation and reductive elimination events.

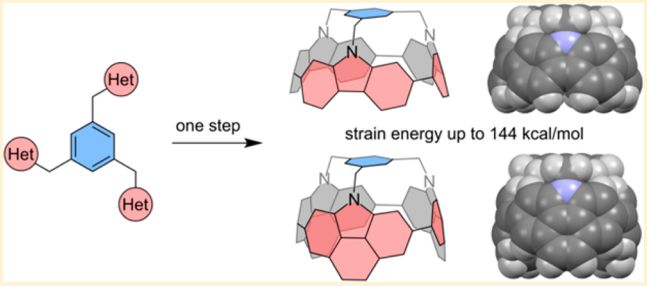

INTRODUCTION

The interest in carbon nanotubes (CNT's),[1] driven by their unique physical properties[2] and potential for practical use,[3] has inspired an extensive search for efficient bottom-up synthetic methods that could lead to materials with perfect structural uniformity. Small end-caps[4] and short ring-like sections[5−7] of single-walled CNT's are currently available through state-of-the-art preparative procedures, which are limited, however, by their multistep character, technical difficulty, and cost. Introduction of strain constitutes the principal challenge in the synthesis of curved aromatic molecules, posing severe energetic and mechanistic restrictions on potentially applicable reactions.[8] The formation of skeletal bonds and introduction of strain are rarely achieved in a single step and feasible synthetic schemes based on solution chemistry often postpone strain induction to the ultimate stage, following the completion of the molecular framework. Examples of the latter approach are found in the synthetic chemistry of [*n*]cycloparaphenylenes ([*n*]CPP's) and their analogues,[5−7] which has flourished since the initial report of Jasti, Bertozzi et al.[9] In the majority of syntheses reported to date by several research groups (for *n* = 5,[10,11] 6,[12] 7,[13−15] 8,[14−17] 9,[9,14,18−21] 10,[14,16,18] 11,[14,18] 12,[9,14,22−24] 13,[18] 14,[18] 15,[20] 16,[18] 18,[9] and 21[20]), the strain was introduced by aromatization of 1,4-cyclohexadiene rings after the formation of an appropriate macrocyclic precursor. An alternative strategy, developed by Yamago et al.,[7,25−28] relies on the construction of multinuclear platinum metallacycles, which are converted into [*n*]CPP's (*n* = 6, 8−13) via the reductive elimination of Pt bridges. While uniquely elegant, this method poses practical problems associated with the stoichiometric use of platinum complexes and other expensive reagents, and with the multistep character of the synthesis. In the Pt-based strategy, the construction of the strained biaryl linkage requires three distinct operations (Scheme 1): activation of a haloarene via formal metal−halogen exchange (1. MHE), transmetalation to a platinacycle intermediate (2. TM), and reductive elimination (3. RE) induced by ligand exchange or oxidation. Depending on a particular formulation, the whole sequence may require from three to five steps and up to four reaction pots.[25−27,29,30]

Scheme 1. Homocoupling Reactions Induced by Group 10 Metals As a Macrocyclization and Strain-Building Synthetic Device[a]

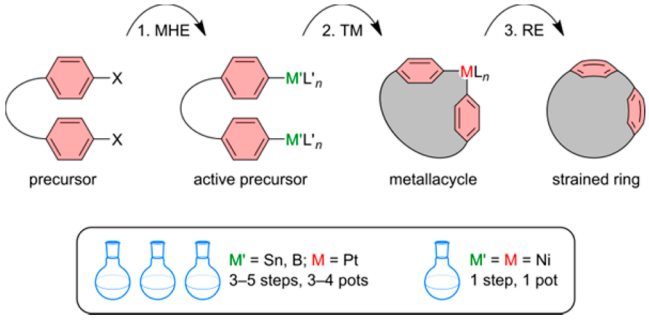

[a]Abbreviations: MHE, metal−halogen exchange; TM, transmetalation; RE, reductive elimination.

Ni[0]-mediated homocouplings of haloarenes[31] provide an efficient contemporary alternative to the classic Ullmann synthesis.[32] The mechanistic layout of these reactions,[33−38] which includes metalation, transmetalation, and reductive

Received: November 21, 2014
Published: December 25, 2014

DOI: 10.1021/ja511951x
J. Am. Chem. Soc. 2015, 137, 1643−1649

Scheme 2. Self-Templated Synthesis of 2a and 2b[a]

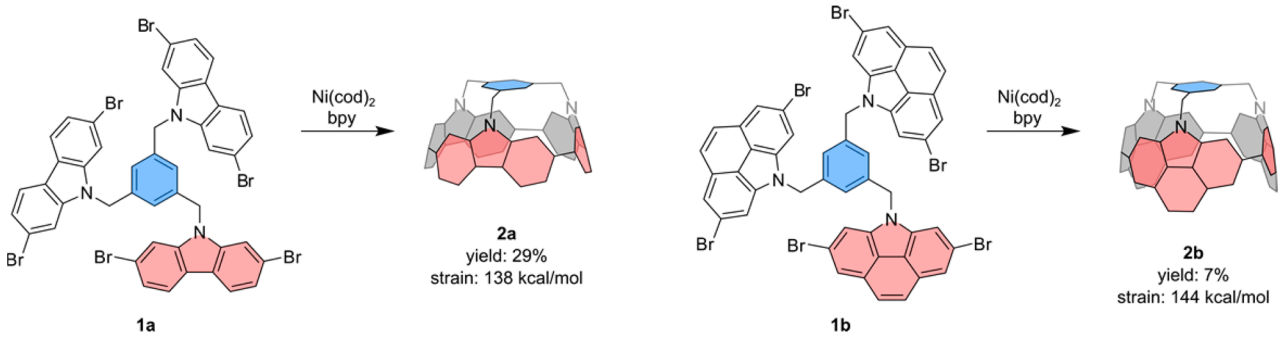

[a]Abbreviations: cod, 1,5-cyclooctadiene; bpy, 2,2′-bipyridyl. In the structures of the products, formal double bonds are omitted for clarity.

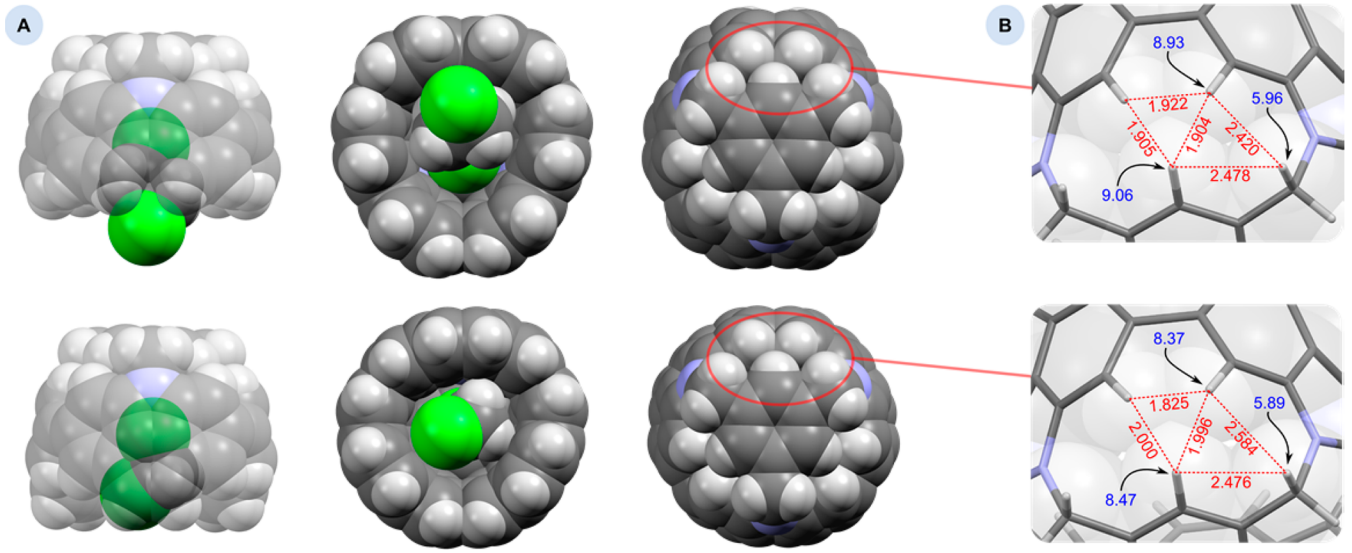

Figure 1. (A) Molecular structures of **2a** (top) and **2b** (bottom) observed in the solid state. Guest molecules of 1,2-dichloroethane (**2a**) and dichloromethane (**2b**) are shown in the figure. (B) Steric interactions in the 13-membered rings of **2a** and **2b** (DFT geometries, distances in Å, red labels) and selected ^{1}H NMR shifts (ppm, blue labels).

elimination steps, parallels Yamago's Pt-based strategy while offering the essential advantage of a single-step procedure (Scheme 1). The utility of the Ni^0 homocoupling as a cyclization tool was recognized early,[39] and it has since been used for the synthesis of diverse macrocyclic structures.[11,23,40−47] Interestingly, strained products could be obtained in direct (one-molecule) macrocyclizations, with reported examples including a macrocyclic disulfone[40] and a partly conjugated precursor to [5]cycloparaphenylene.[11] In contrast, all Ni^0-mediated cyclooligomerizations reported to date led to products with insignificant strain.[23,41,44,45] The desired combination of strain induction with multiple C−C couplings may be difficult to achieve in a single-step cyclooligomerization because it requires proper timing of multiple transmetalation and RE events. However, a cascade of intramolecular strain-inducing couplings can be effected on appropriately designed multifunctional precursors, as evidenced by our recent synthesis of chrysaorole, a carbazole-based bowl-shaped molecule,[8,46] and the preparation of phenylene bicyclophanes by Höger et al.[47] In those two approaches, the estimated increase of internal strain ranged from 18 to 38 kcal/mol per C−C coupling. While the mechanistic aspect of those reactions has not been discussed, their success likely hinged on the self-templating effect provided by partial preorganization of the rigid precursors. The above results suggest that judicious precursor design may be a key to efficient, one-step syntheses of highly distorted aromatic structures.

RESULTS AND DISCUSSION

Synthesis and Structure. In our search for self-templated syntheses of strained molecules,[46,48] we turned our attention to compound **1a** (Scheme 2), which was prepared in one step from commercially available starting materials. Because of its flexible structure, **1a** did not initially seem a suitable self-templating precursor. We were therefore delighted to find that **1a** reacted successfully with the $Ni(cod)_2$/bpy reagent to produce the triply coupled product, **2a**. Under optimized conditions, which involve heating with 9 equiv of Ni^0 in N,N-dimethylformamide (24 h, 100 °C), compound **2a** was isolated in 29% yield after chromatographic workup. Pure **2a** is a reddish solid, soluble in dichloromethane, and shows sufficient stability in solution to enable routine analytical work.

The structure of **2a** was confirmed in the crystal by means of an X-ray diffraction analysis (Figure 1A) and was further explored using gas-phase DFT calculations. The molecule of **2a** contains three strongly bent carbazole subunits that are directly connected via their 2,7 positions to form a macrocyclic sidewall that can be described as [3]cyclo(2,7)carbazole. The

DOI: 10.1021/ja511951x
J. Am. Chem. Soc. 2015, 137, 1643−1649

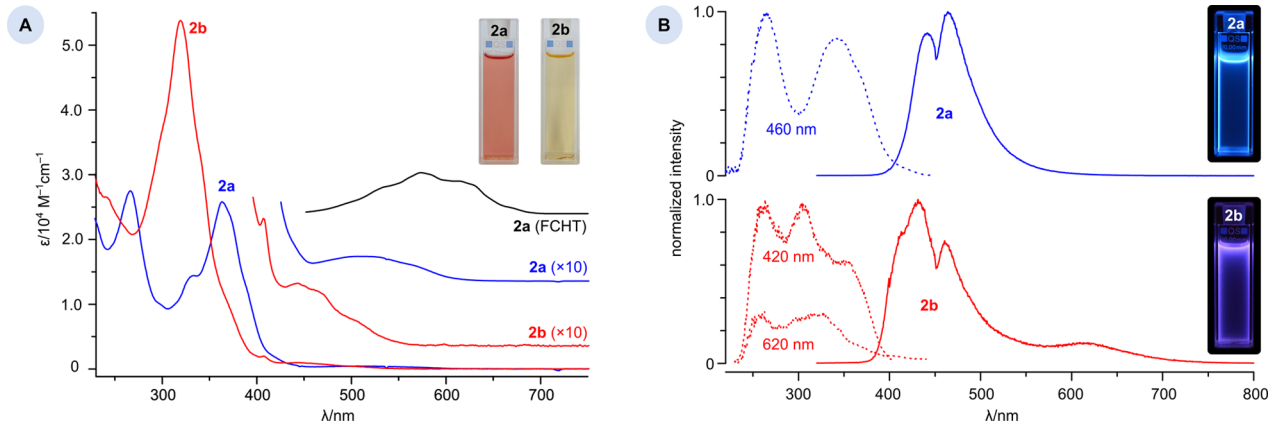

Figure 2. (A) Electronic spectra of **2a** and **2b** (CH_2Cl_2, 293 K). A Franck–Condon-Herzberg–Teller simulation (FCHT) for the lowest energy electronic transition of **2a** is shown in black. (B) Fluorescence emission and excitation spectra (solid and dotted lines, respectively, in CH_2Cl_2, excitation wavelength 310 nm).

connecting bonds are elongated relative to typical C(sp^2)–C(sp^2) distances (1.513 Å X-ray average, 1.510 Å DFT). The sidewall is capped with a benzene ring that is attached to the carbazole nitrogens by means of three methylene groups. The presence of the cap in **2a** creates a rigid bowl-shaped motif, which in spite of obvious structural differences bears a striking resemblance to carbon nanotube end-caps. This similarity is most readily seen in the van der Waals representation of the molecule (Figure 1A), which reveals that the three 13-membered rings in **2a**, which have been completed in the strain-inducing coupling, do not form chemically accessible openings and are in fact tightly closed. Three hydrogens, attached respectively to the benzene cap and two carbazole units, meet at the center of each 13-membered ring at distances much smaller than the sum of the van der Waals radii (1.905–1.922 Å in the DFT model of **2a**, Figure 1B). The cyclocarbazole perimeter in **2a** is shaped into a slightly tapered cavity, with each of the six lateral benzene rings forming an angle of ca. 77° with the basal plane of the molecule. The depth of the cavity measured between the centroid of the cap ring and the centroid of the rim carbons is 4.60 Å, whereas the diameter at the level of rim carbons is 8.60 Å. In the crystal, the interior of **2a** is filled with a molecule of 1,2-dichloroethane, which forms a C···Cl van der Waals contact with the underside of the benzene cap.

The ^{1}H NMR spectrum of **2a**, recorded in CD_2Cl_2 at 300 K, is consistent with the C_{3v} symmetry of the molecule. The carbazole protons of the rim give rise to two signals at 7.57 and 7.25 ppm (a doublet and doublet of doublets). The protons of the upper part of the molecule yield three resonances at 9.06, 8.93, and 5.96 ppm, corresponding respectively to the benzene cap, carbazole 1,8-H positions, and CH_2 bridges. The significantly low-field positions of these signals, which were reproduced in a GIAO–DFT calculation, likely reflect the combination of steric deshielding[49,50] with superimposed ring currents of the unusually aligned aromatic subunits in **2a**. A weak transannular scalar coupling has been identified in the ^{1}H COSY spectrum of **2a** between the signals at 9.06 and 8.93 ppm, which is supposed to have a predominantly through-space character, in view of the topological separation of the corresponding protons (7 bonds).

Compound **2a** contains the embedded motif of [6]CPP, the shortest benzenoid slice of the armchair (6,6) nanotube. It became immediately apparent that larger sections of the (6,6) nanotube might potentially be synthesized by extending our self-templating strategy to precursors with larger fused subunits. The feasibility of such an approach was demonstrated for **1b**, containing three benzo[*def*]carbazole arms, which was converted into the expected capped product **2b** in 7% yield (Scheme 2). The lower coupling efficiency of the latter reaction is supposed to result from the limited solubility of the **1b** precursor and from partial decomposition of the product during workup. The identity of **2b** was unambiguously confirmed by means of standard analytical methods. As in the case of **2a**, all ^{1}H and ^{13}C signals were assigned on the basis of correlation data and the shifts were reproduced using a GIAO calculation. The solid-state geometry of **2b** reveals a cavity with a depth of 5.90 Å, sufficient to enclose an entire dichloromethane molecule. The cavity is deeper than that found in the recently reported end-cap fragment of (5,5)CNT[4] (5.16 Å). In comparison with **2a**, **2b** has a smaller base diameter (8.14 Å), identical with the value estimated[51] for the (6,6)CNT. The contraction of the open end of the **2b** nanotube relative to **2a** results in a tapered shape of the sidewalls (Figure 1A) and partially relieves the steric congestion in the 13-membered rings. The key nonbonded H···H distances inside those rings increase by only ca. 0.1 Å, but this small change leads to a remarkable upfield relocation of the corresponding ^{1}H NMR signals in comparison with **2a** (8.46 and 8.37 ppm, Figure 1B).

Using a homodesmotic reaction scheme based on the conversion of **1a** into **2a**, an internal strain of 138 kcal/mol was estimated for the latter structure (gas-phase DFT energy). This value is higher than the analogous energies calculated for [6]CPP and [5]CPP relative to 4,4′-dibromobiphenyl (98 and 119 kcal/mol, respectively, in good agreement with earlier estimates[10–12,52]). Structural factors contributing to the unusually large strain found in **2a** are thought to include (a) the greater resistance of carbazole subunits toward bending relative to individual benzene rings, (b) limited conformational freedom of **2a** in comparison to CPP's, which leads to increased H···H repulsions between adjacent carbazole fragments, and (c) steric congestion caused by capping. The latter contribution was estimated to be 19 kcal/mol relative to a cap-free analogue of **2a** containing three benzyl groups. The formation of **2b** from **1b** is associated with a strain increase that is higher by 6 kcal/mol than the value obtained for **2a**. However, the above calculation ignores the internal strain of the benzo[def]-carbazole subunits, which stems from the nonbenzenoid *peri*

DOI: 10.1021/ja511951x
J. Am. Chem. Soc. 2015, 137, 1643–1649

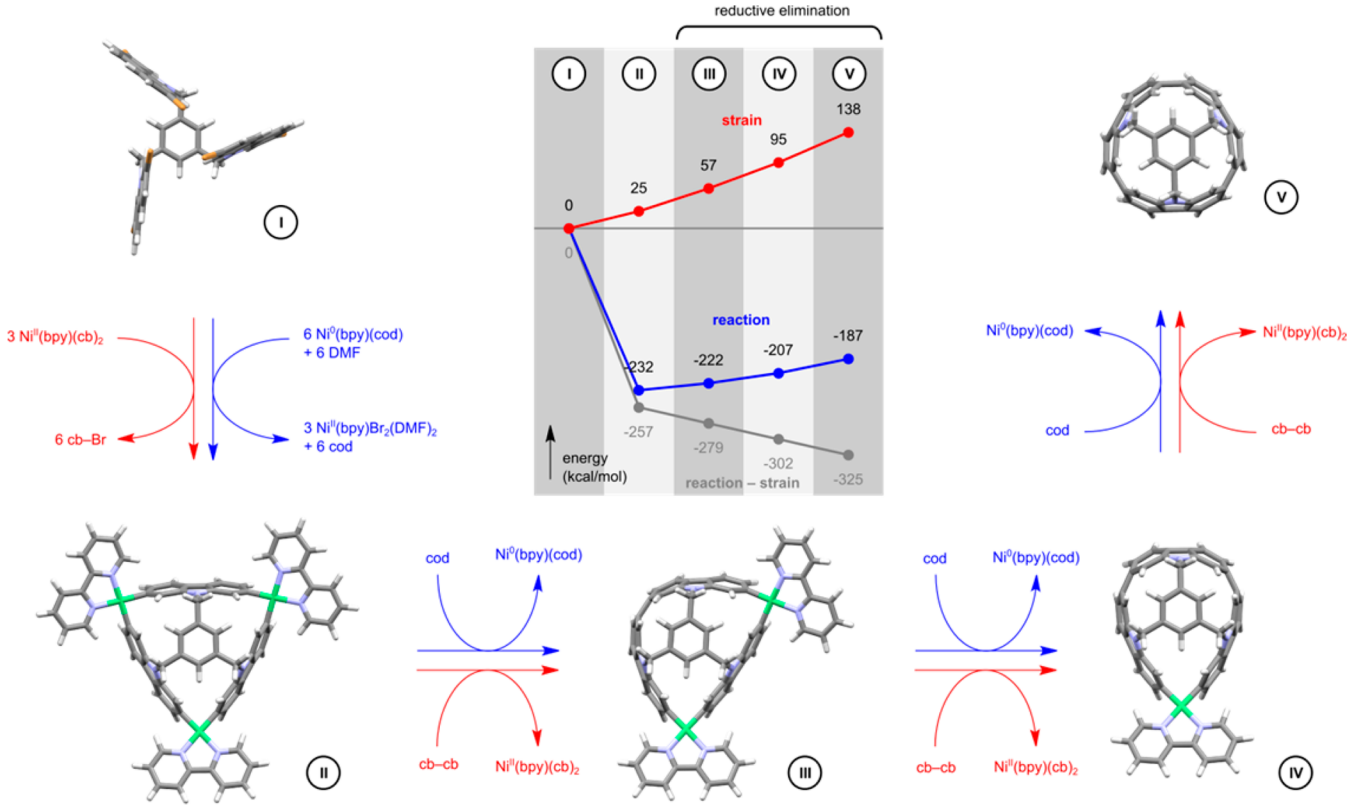

Figure 3. Theoretical modeling of the templated cyclization reaction leading to **2a**. bpy = 2,2′-bipyridyl, cod = 1,5-cyclooctadiene, DMF = *N*,*N*-dimethylformamide, cb =2-carbazolyl. Energetics of the Ni-mediated homocoupling reaction (B3LYP/6-31G(d,p), in vacuo) are calculated for the reagent system shown in blue. Strain energies correspond to the homodesmotic reaction sequence shown in red.

fusion of the four constituent rings. The inclusion of the latter energy component leads to a much larger strain difference between **2b** and **2a**, exceeding 50 kcal/mol. The strain contribution due to capping is lower in **2b** (16 kcal/mol), in line with the observed relaxation of nonbonded distances in the 13-membered rings.

Electronic Structure. The voltammetric analysis of **2a** revealed two electrochemically quasireversible one-electron oxidations at 57 and 183 mV (vs the ferrocene/ferrocenium couple), with no reduction events detectable down to −2400 mV. The electrochemical oxidation of **2b** starts at ca. 120 mV and is essentially irreversible. The process is associated with the deposition of a blue-colored, highly conductive material on the working electrode, which retains its properties when transferred to a fresh solution of supporting electrolyte.

In contrast to CPP's, which exhibit a single absorption band in the UV region of the electronic spectrum, compound **2a** shows several intense absorptions, with two major maxima at 266 and 363 nm ($\varepsilon = 2.7 \times 10^4$ and 2.6×10^4 M^{-1} cm^{-1}, Figure 2A). These UV bands are accompanied by a significantly weaker broad feature, which has measurable intensity up to ca. 660 nm (λ_{max} = 507 nm, $\varepsilon = 3.8 \times 10^2$ M^{-1} cm^{-1}), and is responsible for the red color of the compound. A similar weak absorption, ascribed to the symmetry-forbidden HOMO−LUMO transition, was also observed in [5]CPP and [6]-CPP.[10,12] **2b** also exhibits a similar low-intensity absorption in the visible region, which is unexpectedly shifted to shorter wavelengths (λ_{max} = 443 nm, $\varepsilon = 1.2 \times 10^3$ M^{-1} cm^{-1}), as reflected by the orange color observed in solution. However, **2b** shows a single major band in the UV part of the spectrum, with a maximum at 319 nm. Unlike [6]cycloparaphenylene, **2a** shows easily observable blue fluorescence with two emission maxima at ca. 440 and 465 nm (Figure 2B). These values correspond to higher energies than the lowest energy electronic transition, indicating that the emission does not occur from the S_1 state. The fluorescence spectrum of **2b** contains three overlapping bands with a maximum at ca. 431 nm, accompanied by a broad and remarkably intense feature at ca. 630 nm. Fluorescence quantum yields determined for **2a** and **2b** are 0.18 and 0.06, respectively.

The HOMO (H) and LUMO (L) orbitals calculated for **2a** at the B3LYP/6-31G(d,p) level of theory are characterized by near-zero amplitudes on the capping benzene ring. The contributions of the benzene π-system to lower occupied levels (H − 3 to H − 1) are also insignificant. However, large amplitudes on the carbazole and benzene fragments of the molecule are simultaneously observed in the doubly degenerate L + 1 and L + 2 levels. Time-dependent DFT calculations using the Tamm−Dancoff approximation (TDA-DFT) show that excitations to these higher unoccupied orbitals participate in the most intense transitions, indicating that the cap, though not contiguously π-conjugated with the cyclocarbazole sidewall, can have an auxochromic effect on the observed electronic absorptions of **2a**. The calculated TDA spectrum of **2a** corresponds very well with the experimental absorption profile. The predicted energy of this transition is 606 nm, which agrees with the observed absorption edge. For **2b**, TDA correctly yields a single absorption maximum in the ultraviolet region, and the calculated HOMO−LUMO transition (521 nm) is blue-shifted relative to **2a**. Calculated MO levels indicate that upon going from **2a** to **2b**, the interaction between the cap and sidewall parts of the molecule undergoes a qualitative change,

DOI: 10.1021/ja511951x
J. Am. Chem. Soc. 2015, 137, 1643−1649

which is reflected in the altered pattern of higher unoccupied orbitals. As in cycloparaphenylenes, the HOMO−LUMO transitions in **2a** and **2b** are forbidden (f = 0), and their appearance in the experimental spectra can be ascribed to dynamic effects. For both systems, the corresponding absorption bands have low intensity and reveal an incompletely resolved vibronic structure, which was successfully reproduced in a Franck−Condon/Herzberg−Teller calculation performed for **2a** (B3LYP/6-31G(d,p), Figure 2A). The FCHT method underestimates the energy of the 0−0 transition by ca. 0.13 eV relative to the experiment, a difference that can be ascribed to solvent effects.[53]

The above results indicate that the optical properties of **2a** and **2b** are likely to reflect the complex behavior of cycloparaphenylenes revealed by the recent spectroscopic and theoretical work.[54−60] The photoluminescence of [n]CPP's is currently proposed to originate principally from the symmetry-forbidden vibronically activated S_1 state,[57] although emissive contributions from higher excited states[56,58] have also been considered for larger rings. On the basis of the structural analogy between [6]CPP[12] and **2a**, it may be tentatively proposed that the S_1 emission is unobservable in the latter compound because of inefficient vibronic coupling. The fluorescence activity of higher excited states, which is absent in [6]CPP, may then be linked to the presence of the capping unit and nitrogen atoms in **2a**. Interestingly, the vertical $S_2 - S_1$ energy difference is reduced from 0.86 eV in **2a** to 0.40 eV in **2b** (TDA values). Such a change was proposed to enhance the S_1 fluorescence quantum yield in larger CPP's[58] and might lead to the activation of S_1 emission in **2b**. Regardless of the theoretical interpretation, the strikingly different behavior of **2a** and **2b** provides compelling evidence that the luminescent properties of discrete CNT fragments can be tuned not only by changing the tube diameter, as demonstrated by CPP fluorescence, but also by varying the axial length.

Mechanism. In the ArBr/Ni(cod)$_2$/bpy/DMF reagent system,[33,34] used here to make **2a** and **2b**, the coupling has been determined to begin with the oxidative addition of Ni(bpy)(cod)[35,61] to the aryl halide (step 1 in Scheme 1). Subsequent ligand metathesis (step 2)[36,37] produces the bis(aryl) Ni^{II} intermediate and an aryl-free byproduct, recently identified as Ni(bpy)Br$_2$(DMF)$_2$.[38] Ultimately, the biaryl is formed through reductive elimination (step 3, Scheme 1), which is likely induced by the coordination of a cod molecule to Ni^{II}.[62] This last step regenerates one equivalent of the starting Ni^0(bpy)(cod). Using the above mechanism, the coupling of **1a** was investigated computationally in the gas phase (Figure 3, see Supporting Information Table S2 and the accompanying comment for accuracy considerations). DFT calculations provided semiquantitative estimates of total energy changes (blue arrows) and of the internal strain component at each reaction stage (red arrows). The formation of **2a** clearly implies the intermediacy of a triply Ni-bridged intermediate (**II**, Figure 3) because any RE event occurring prior to the completion of the Ni_3 metallacycle in **II** would move apart the termini of the growing oligocarbazole, radically lowering the probability of the ultimate Ni^{II} bridging. Interestingly, the formation of **II** generates 25 kcal/mol of internal strain (18% of the total strain in **2a**), which is visually manifested by the bending of carbazole subunits in the DFT structure. Nevertheless, the above process is predicted to be strongly exothermic, yielding an energy gain of 232 kcal/mol in the gas phase (ca. 39 kcal/mol per C−Ni bond). Intermediate **II** is converted into **2a** in three consecutive RE steps (via species **III** and **IV**), providing increasing individual strain contributions of 32, 38, and 43 kcal/mol. In the strain-free reference system, the RE step is exothermic but the reaction energy (ca. 23 kcal/mol per C−C bond) is not sufficient to overcome the strain incurred by **III**, **IV**, and **2a** at each elimination stage. Consequently, the overall conversion of **II** into **2a** becomes endothermic by 35 kcal/mol.

Reported kinetic data show that, for unstrained biaryl products, the rate-determining step of the homocoupling corresponds to the transmetalation event (TM) that leads to the bis(aryl)nickel complex,[33,37] suggesting that, in general, the MHE and RE steps should be appreciably faster. This kinetic picture is apparently altered in the present case because for an efficient formation of the Ni_3 metallacycle **II**, the fastest RE step must be slower than the slowest TM. Rates of productive reaction pathways leading to **2a** or **2b**, therefore, are presumed to be determined by reductive eliminations rather than transmetalations. Arguably, the RE from intermediates **II**−**IV** may be slowed down by the growing internal strain, which should affect the respective transition states. Simultaneously, transmetalations leading to **II** are intramolecular and may be faster than intermolecular TM's at practicable reactant concentrations. The above assumptions are consistent with the observed stoichiometry of the reaction. Typically, the use of 1 equiv of Ni^0 per C−C bond is sufficient to achieve almost complete coupling of simple reactants.[33,63] However, the reaction of **1a** with 3.3 equiv of Ni(cod)$_2$ yields only traces of **2a**. Reactions with a stoichiometric amount of Ni(cod)$_2$ must involve recycling of the Ni^0 species released after reductive elimination. The synthesis of **2a** relies on the temporal separation of the transmetalation and elimination stages, which is incompatible with Ni^0 recycling. To form all three C−Ni−C bridges before any elimination occurs, one needs at least 6 equiv of the Ni^0 reagent per molecule of **1a**. Yields of **2a** are also lowered when free cod (10 equiv) is added to the reaction. This observation is consistent with the proposed mechanism because increasing cod concentration is known to slow down transmetalation[33] and may be expected to enhance elimination rates.[62]

■ SUMMARY AND CONCLUSION

The self-templated synthesis of heteroaromatic nanotube end-caps presented herein shifts the limit of strain induction achievable in aromatic systems through the use of solution chemistry. The new strategy combines skeletal assembly and strain build-up into a single step, enabling concise preparation of complex aromatic structures from simply functionalized starting materials. By extending the fusion pattern in appropriately designed multiarm precursors, it is possible to construct three-dimensional π-conjugated systems with deep, rigid cavities. This potential, combined with unusual electronic structures of the resulting systems, makes them of interest as prospective receptors, elements of supramolecular architecture, and materials for organic electronics. In a broader perspective, combining the present self-templated synthesis with removal of the capping unit may be envisaged as a size-selective route to hoop-shaped molecules. Further exploration, which is ongoing in our laboratory, is aimed at expanding the scope of the present strategy and providing deeper mechanistic insight into the underlying organometallic chemistry.

DOI: 10.1021/ja511951x
J. Am. Chem. Soc. 2015, 137, 1643−1649

■ ASSOCIATED CONTENT

Supporting Information

Experimental procedures and analytical data for all new compounds. Additional NMR and mass spectra, and electrochemistry data. X-ray data for **2a** and **2b** (CIF). Computational data tables, figures, and Cartesian coordinates (PDB). This material is available free of charge via the Internet at http://pubs.acs.org.

■ AUTHOR INFORMATION

Corresponding Author

marcin.stepien@chem.uni.wroc.pl

Notes

The authors declare no competing financial interest.

■ ACKNOWLEDGMENTS

Financial support from the National Science Center (M.S., Grant 2012/07/E/ST5/00781), Foundation for Polish Science (D.M., START Programme), and European Union ("Human Capital" scholarship to D.M.) is kindly acknowledged. Quantum chemical calculations were performed in the Wrocław Center for Networking and Supercomputing. We thank Joanna Cybińska for help with fluorescence measurements.

■ REFERENCES

(1) Iijima, S. *Nature* **1991**, *354*, 56−58.
(2) *Carbon Nanotubes and Related Structures: Synthesis, Characterization, Functionalization, and Applications*; Guldi, D. M., Martín, N., Eds.; Wiley-VCH: Weinheim, Germany, 2010.
(3) Volder, M. F. L. D.; Tawfick, S. H.; Baughman, R. H.; Hart, A. J. *Science* **2013**, *339*, 535−539.
(4) Scott, L. T.; Jackson, E. A.; Zhang, Q.; Steinberg, B. D.; Bancu, M.; Li, B. *J. Am. Chem. Soc.* **2012**, *134*, 107−110.
(5) Hirst, E. S.; Jasti, R. *J. Org. Chem.* **2012**, *77*, 10473−10478.
(6) Omachi, H.; Segawa, Y.; Itami, K. *Acc. Chem. Res.* **2012**, *45*, 1378−1389.
(7) Yamago, S.; Kayahara, E.; Iwamoto, T. *Chem. Rec.* **2014**, *14*, 84−100.
(8) Stępień, M. *Synlett* **2013**, *24*, 1316−1321.
(9) Jasti, R.; Bhattacharjee, J.; Neaton, J. B.; Bertozzi, C. R. *J. Am. Chem. Soc.* **2008**, *130*, 17646−17647.
(10) Evans, P. J.; Darzi, E. R.; Jasti, R. *Nat. Chem.* **2014**, *6*, 404−408.
(11) Kayahara, E.; Patel, V. K.; Yamago, S. *J. Am. Chem. Soc.* **2014**, *136*, 2284−2287.
(12) Xia, J.; Jasti, R. *Angew. Chem., Int. Ed.* **2012**, *51*, 2474−2476.
(13) Sisto, T. J.; Golder, M. R.; Hirst, E. S.; Jasti, R. *J. Am. Chem. Soc.* **2011**, *133*, 15800−15802.
(14) Darzi, E. R.; Sisto, T. J.; Jasti, R. *J. Org. Chem.* **2012**, *77*, 6624−6628.
(15) Sibbel, F.; Matsui, K.; Segawa, Y.; Studer, A.; Itami, K. *Chem. Commun.* **2014**, *50*, 954−956.
(16) Xia, J.; Bacon, J. W.; Jasti, R. *Chem. Sci.* **2012**, *3*, 3018−3021.
(17) Tran-Van, A.-F.; Huxol, E.; Basler, J. M.; Neuburger, M.; Adjizian, J.-J.; Ewels, C. P.; Wegner, H. A. *Org. Lett.* **2014**, *16*, 1594−1597.
(18) Ishii, Y.; Nakanishi, Y.; Omachi, H.; Matsuura, S.; Matsui, K.; Shinohara, H.; Segawa, Y.; Itami, K. *Chem. Sci.* **2012**, *3*, 2340−2345.
(19) Nishiuchi, T.; Feng, X.; Enkelmann, V.; Wagner, M.; Müllen, K. *Chem.−Eur. J.* **2012**, *18*, 16621−16625.
(20) Golling, F. E.; Quernheim, M.; Wagner, M.; Nishiuchi, T.; Müllen, K. *Angew. Chem., Int. Ed.* **2014**, *53*, 1525−1528.
(21) Huang, C.; Huang, Y.; Akhmedov, N. G.; Popp, B. V.; Petersen, J. L.; Wang, K. K. *Org. Lett.* **2014**, *16*, 2672−2675.
(22) Takaba, H.; Omachi, H.; Yamamoto, Y.; Bouffard, J.; Itami, K. *Angew. Chem., Int. Ed.* **2009**, *48*, 6112−6116.
(23) Segawa, Y.; Miyamoto, S.; Omachi, H.; Matsuura, S.; Šenel, P.; Sasamori, T.; Tokitoh, N.; Itami, K. *Angew. Chem., Int. Ed.* **2011**, *50*, 3244−3248.
(24) Sisto, T. J.; Tian, X.; Jasti, R. *J. Org. Chem.* **2012**, *77*, 5857−5860.
(25) Yamago, S.; Watanabe, Y.; Iwamoto, T. *Angew. Chem., Int. Ed.* **2010**, *49*, 757−759.
(26) Iwamoto, T.; Watanabe, Y.; Sakamoto, Y.; Suzuki, T.; Yamago, S. *J. Am. Chem. Soc.* **2011**, *133*, 8354−8361.
(27) Kayahara, E.; Sakamoto, Y.; Suzuki, T.; Yamago, S. *Org. Lett.* **2012**, *14*, 3284−3287.
(28) Kayahara, E.; Iwamoto, T.; Suzuki, T.; Yamago, S. *Chem. Lett.* **2013**, *42*, 621−623.
(29) Hitosugi, S.; Yamasaki, T.; Isobe, H. *J. Am. Chem. Soc.* **2012**, *134*, 12442−12445.
(30) Matsuno, T.; Kamata, S.; Hitosugi, S.; Isobe, H. *Chem. Sci.* **2013**, *4*, 3179−3183.
(31) Semmelhack, M. F.; Helquist, P. M.; Jones, L. D. *J. Am. Chem. Soc.* **1971**, *93*, 5908−5910.
(32) Hassan, J.; Sévignon, M.; Gozzi, C.; Schulz, E.; Lemaire, M. *Chem. Rev.* **2002**, *102*, 1359−1470.
(33) Yamamoto, T.; Wakabayashi, S.; Osakada, K. *J. Organomet. Chem.* **1992**, *428*, 223−237.
(34) Yamamoto, T. *Bull. Chem. Soc. Jpn.* **2010**, *83*, 431−455.
(35) Abla, M.; Yamamoto, T. *Bull. Chem. Soc. Jpn.* **1999**, *72*, 1255−1261.
(36) Matsumoto, H.; Inaba, S.; Rieke, R. D. *J. Org. Chem.* **1983**, *48*, 840−843.
(37) Osakada, K.; Yamamoto, T. *Coord. Chem. Rev.* **2000**, *198*, 379−399.
(38) Asakura, H.; Shishido, T.; Tanaka, T. *J. Phys. Chem. A* **2012**, *116*, 4029−4034.
(39) Semmelhack, M. F.; Ryono, L. S. *J. Am. Chem. Soc.* **1975**, *97*, 3873−3875.
(40) Colquhoun, H. M.; Zhu, Z.; Williams, D. J. *Org. Lett.* **2001**, *3*, 4031−4034.
(41) Jung, S.-H.; Pisula, W.; Rouhanipour, A.; Räder, H. J.; Jacob, J.; Müllen, K. *Angew. Chem., Int. Ed.* **2006**, *45*, 4685−4690.
(42) Pisula, W.; Kastler, M.; Yang, C.; Enkelmann, V.; Müllen, K. *Chem.−Asian J.* **2007**, *2*, 51−56.
(43) Simon, S. C.; Schmaltz, B.; Rouhanipour, A.; Räder, H. J.; Müllen, K. *Adv. Mater.* **2009**, *21*, 83−85.
(44) Nakanishi, W.; Matsuno, T.; Ichikawa, J.; Isobe, H. *Angew. Chem., Int. Ed.* **2011**, *50*, 6048−6051.
(45) Nakanishi, W.; Yoshioka, T.; Taka, H.; Xue, J. Y.; Kita, H.; Isobe, H. *Angew. Chem., Int. Ed.* **2011**, *50*, 5323−5326.
(46) Myśliwiec, D.; Stępień, M. *Angew. Chem., Int. Ed.* **2013**, *52*, 1713−1717.
(47) Ohlendorf, G.; Mahler, C. W.; Jester, S.-S.; Schnakenburg, G.; Grimme, S.; Höger, S. *Angew. Chem., Int. Ed.* **2013**, *52*, 12086−12090.
(48) Kondratowicz, M.; Myśliwiec, D.; Lis, T.; Stępień, M. *Chem.−Eur. J.* **2014**, *20*, 14981−14985.
(49) Cheney, B. V. *J. Am. Chem. Soc.* **1968**, *90*, 5386−5390.
(50) Zong, J.; Mague, J. T.; Pascal, R. A. *J. Am. Chem. Soc.* **2013**, *135*, 13235−13237.
(51) Dresselhaus, M. S.; Dresselhaus, G.; Eklund, P. C. *Science of Fullerenes and Carbon Nanotubes: Their Properties and Applications*; Academic Press: New York, 1996.
(52) Segawa, Y.; Omachi, H.; Itami, K. *Org. Lett.* **2010**, *12*, 2262−2265.
(53) Dierksen, M.; Grimme, S. *J. Chem. Phys.* **2004**, *120*, 3544−3554.
(54) Segawa, Y.; Fukazawa, A.; Matsuura, S.; Omachi, H.; Yamaguchi, S.; Irle, S.; Itami, K. *Org. Biomol. Chem.* **2012**, *10*, 5979−5984.
(55) Nishihara, T.; Segawa, Y.; Itami, K.; Kanemitsu, Y. *J. Phys. Chem. Lett.* **2012**, *3*, 3125−3128.
(56) Camacho, C.; Niehaus, T. A.; Itami, K.; Irle, S. *Chem. Sci.* **2013**, *4*, 187−195.

DOI: 10.1021/ja511951x
J. Am. Chem. Soc. 2015, 137, 1643−1649

(57) Adamska, L.; Nayyar, I.; Chen, H.; Swan, A. K.; Oldani, N.; Fernandez-Alberti, S.; Golder, M. R.; Jasti, R.; Doorn, S. K.; Tretiak, S. *Nano Lett.* **2014**, *14*, 6539−6546.
(58) Reddy, V. S.; Camacho, C.; Xia, J.; Jasti, R.; Irle, S. *J. Chem. Theory Comput.* **2014**, *10*, 4025−4036.
(59) Hines, D. A.; Darzi, E. R.; Jasti, R.; Kamat, P. V. *J. Phys. Chem. A* **2014**, *118*, 1595−1600.
(60) Nishihara, T.; Segawa, Y.; Itami, K.; Kanemitsu, Y. *Chem. Sci.* **2014**, *5*, 2293−2296.
(61) Dinjus, E.; Walther, D.; Kaiser, J.; Sieler, J.; Ngoc Thanh, N. *J. Organomet. Chem.* **1982**, *236*, 123−130.
(62) Yamamoto, T.; Yamamoto, A.; Ikeda, S. *J. Am. Chem. Soc.* **1971**, *93*, 3350−3359.
(63) Yamamoto, T.; Morita, A.; Miyazaki, Y.; Maruyama, T.; Wakayama, H.; Zhou, Z. H.; Nakamura, Y.; Kanbara, T.; Sasaki, S.; Kubota, K. *Macromolecules* **1992**, *25*, 1214−1223.

DOI: 10.1021/ja511951x
J. Am. Chem. Soc. 2015, 137, 1643−1649